

WL-TM-97-3065



**DEVELOPMENT OF NON-LINEAR,
LOW-SPEED AERODYNAMIC
MODEL FOR THE F-16/VISTA**

**Jacob Kay
John N. Ralston
Stanley F. Lash**

**Bihrlle Applied Research, Inc.
400 Jericho Turnpike
Jericho, NY 11753**

AUGUST 1997

FINAL REPORT FOR 1 MAY 1997 - 31 MAY 1997

Approved for public release; distribution unlimited

DTIC QUALITY INSPECTED 3

**FLIGHT DYNAMICS DIRECTORATE
WRIGHT LABORATORY
AIR FORCE MATERIEL COMMAND
WRIGHT-PATTERSON AFB OH 45433-7662**

19970804 033

**THIS PAPER IS DECLARED A WORK OF THE U.S. GOVERNMENT AND AS SUCH IS
NOT SUBJECT TO COPYRIGHT PROTECTION IN THE UNITED STATES.**

REPORT DOCUMENTATION PAGE

Form Approved
OMB No. 0704-0188

1. REPORT DOCUMENTATION PAGE. The burden for this collection of information is estimated to average 1 hour per response, including the time for reviewing instructions, searching existing data sources, gathering and maintaining the data needed, and completing and reviewing the collection of information. Send comments regarding this burden estimate or any other aspect of this collection of information, including suggestions for reducing this burden, to Washington Headquarters Services, Directorate for Information Operations and Reports, 1215 Jefferson Davis Highway, Suite 1202, Arlington, VA 22202-4302, and to the Office of Management and Budget, Paperwork Reduction Project (0704-0188), Washington, DC 20503.

1. REPORT DATE (Leave Blank) 2. REPORT DATE AUG 1997 3. REPORT TYPE AND DATES COVERED FINAL 1 MAY 1997 - 31 MAY 1997

4. TITLE (or SUBTITLE) DEVELOPMENT OF NON-LINEAR, LOW-SPEED AERODYNAMIC MODEL FOR THE F-16/VISTA

5. FUNDING NUMBERS
C
PE 62
PR 2403
TA 05
WU 96

6. AUTHOR(S)
JACOB KAY
JOHN N. RALSTON
STANLEY F. LASH

7. PERFORMING ORGANIZATION
REPORT NUMBER

8. SPONSORING/MONITORING AGENCY REPORT NUMBER
WL-TM-97-3065

9. SPONSORING/MONITORING AGENCY NAME(S) AND ADDRESS(ES)
FLIGHT DYNAMICS DIRECTORATE
WRIGHT LABORATORY
AIR FORCE MATERIEL COMMAND
WRIGHT PATTERSON AFB OH 45433-7562

10. SPONSORING/MONITORING AGENCY NAME(S) AND ADDRESS(ES)
FLIGHT DYNAMICS DIRECTORATE
WRIGHT LABORATORY
AIR FORCE MATERIEL COMMAND
WRIGHT PATTERSON AFB OH 45433-7562
POC: STANLEY LASH, WL/FIGC (937) 255-8275

11. SUBJECT KEY WORDS
CONFERENCE PAPER: ATMOSPHERIC FLIGHT
MECHANICS CONFERENCE, AIAA, NEW ORLEANS, LA. 11 AUG 97

12a. SUBJECT APPROVABILITY STATEMENT
APPROVED FOR PUBLIC RELEASE; DISTRIBUTION IS
UNLIMITED.

12b. DISTRIBUTION CODE

13. ABSTRACT (about 300 words)
A NEW LOW-SPEED AERODYNAMIC DATABASE FOR THE F-16/VISTA WAS DEVELOPED FROM LOW-SPEED DATA SETS OBTAINED FROM NASA LANGLEY'S FACILITIES. THIS NEW MODEL WAS DESIGNED TO BE CONTINUOUS FROM -80 DEGREES TO +90 DEGREES ANGLE OF ATTACK, -30 DEGREES TO +30 DEGREES OF SIDESLIP, AND TO INCORPORATE ALL SIDESLIP AND CONTROL EFFECTIVENESS INTERACTIONS IN A FULLY NON-LINEAR STRUCTURE. THIS PAPER FIRST REVIEWS THE MODEL STRUCTURE AND DOCUMENTS THE AERODYNAMIC DATA SOURCE USED TO ASSEMBLE THE DATA. THE SUBSEQUENT DISCUSSION EXAMINES THE METHODOLOGY USED TO CORRELATE AND VALIDATE THE MODEL AGAINST FLIGHT TEST DATA AS WELL AS THE RATIONALES FOR THE MODEL CHANGES.

14. NUMBER OF PAGES
14

15. PRICE CODE
16. PRICE CODE

17. SECURITY CLASSIFICATION
UNCLASSIFIED

18. SECURITY CLASSIFICATION
UNCLASSIFIED

19. SECURITY CLASSIFICATION
UNCLASSIFIED

20. LIMITATION
SAR

DEVELOPMENT OF NON-LINEAR, LOW-SPEED AERODYNAMIC MODEL FOR THE F-16/VISTA

Jacob Kay* and John N. Ralston†
Birrle Applied Research, Inc. Hampton, VA

Stanley F. Lash‡
Wright Laboratory, WPAFB, OH

Summary

A new low-speed aerodynamic database for the F-16/VISTA was developed from low-speed data sets obtained from NASA Langley's 30x60 facility and 20-ft vertical wind tunnel and NASA Ames' 12-ft pressure tunnel. This new model was designed to be continuous from -80° to $+90^\circ$ angle of attack, -30° to $+30^\circ$ of sideslip, and to incorporate all sideslip and control effectiveness interactions in a fully non-linear structure. The aerodynamic data set also includes wind-axis and body-axis damping terms and is configured to utilize these data separately for high-fidelity modeling of dynamic conditions. The purpose of this effort is to demonstrate the benefits of a completely nonlinear aerodynamic data base to capture the dependencies that occur while maneuvering at high angle of attack. This model was validated against a set of high angle of attack flight data from the F-16 VISTA/MATV flight test program. Minimal refinements to the data set were required to produce an excellent correlation between the simulation model and the flight test results for maneuvers in and above the stall regime.

Introduction

With extensive backgrounds in modeling nonlinear aerodynamic characteristics, Bihrlle Applied Research was tasked by the Wright Lab Flight Control Division to develop a new F-16 aerodynamic model with the philosophy of incorporating all known nonlinear static and dynamic characteristics from available wind tunnel data. This new F-16 (and VISTA) low-speed simulation aerodynamic model was developed to assess the impact of incorporating these non-linear effects on high-angle of attack simulation to analyze the VISTA/MATV flight test data and was developed to be amenable to database updates. This was accomplished by applying the philosophy of using all available wind tunnel data and letting the test data functionalities and all interactions be modeled as continuous functions in the simulation data set. This low-speed model is entirely non-linear

and continuous from -80° to $+90^\circ$ angle of attack with non-symmetric mechanization of sideslip effects for the basic aircraft characteristics. All sideslip and control surface effectiveness interactions were modeled as dictated by the wind tunnel data. While benefiting from hindsight that earlier models lacked, it was hoped that by starting with a carefully structured non-linear model merging the best available data would result in a simulation that would more closely model the VISTA's post-stall characteristics.

This paper first reviews the model structure and documents the aerodynamic data source used to assemble the data set. The subsequent discussion examines the methodology used to correlate and validate the model against flight test data as well as the rationales for the model changes. Finally, simulation runs using flight-recorded stick inputs will be used to demonstrate the low-speed model's fidelity in the stall and post stall region.

Low-Speed Aerodynamic Model

The basic static F-16's low-speed

aerodynamic model was assembled primarily from the NASA Langley 30x60 low-speed tests for the upright angle of attack range and the NASA Ames 12-ft pressure tunnel data for the inverted characteristics as illustrated in Figure 1. The 30x60 wind tunnel data range extended from -5° to $+60^\circ$ angle of attack and out to $\pm 20^\circ$ of sideslip. Because of the known non-linear variations in the aerodynamic characteristics beyond 20° of sideslip, the low-speed wind tunnel data from the Langley's 20-ft vertical wind tunnel were used to extend the sideslip functionality to $\pm 30^\circ$ for all six body-axis force and moment coefficients. In addition, the same data set was used to extend the angle of attack from 60° to 90° .

For the 30x60 upright wind tunnel data set, control effectiveness runs were conducted on the basic F-16 configuration with primarily full trailing edge deflections. Additionally, since a comprehensive set of

* Engineer

† Engineering Manager

‡ Principal Scientist, Flight Dynamics Directorate, Control Dynamics Branch

control surface deflections had been tested at the NASA Langley's 20-ft wind tunnel, these data (from Reference 1 to 5) were used to define the nonlinear variation in control authority as a function of surface deflections and combined with control effectiveness data from the 30x60 data to result in a very high-fidelity control effectiveness model. NASA Ames' inverted wind tunnel data were used to define the control effectiveness model at inverted angles of attack. Both the Ames inverted and the Langley data sets exhibited sideslip dependencies, and the characteristics were incorporated as well.

While the previous aerodynamic data sets incorporate only linearized body-axis damping derivatives to model the F-16's dynamic characteristics, the new low-speed model use both body-axis damping derivatives as well as wind axis rotary data. These data were mechanized separately and combined in the simulation using the techniques proposed by Kalviste (Reference 6). For the wind-axis damping terms, traditionally referred to as the rotary balance data, the extensive test results from NASA Langley 20-ft Vertical Tunnel were used. Nonlinear variations in the forces and moments due to rotation rates, sideslip angles and control surface deflections were also mechanized in the model. NASA Langley's 30x60 forced oscillation rig provided the data for the body-axis damping derivatives.

To account for the differences in the external features of the VISTA configuration, incremental aerodynamic effects were applied to the baseline F-16 data base to model the VISTA aerodynamic characteristics. Rather than incorporating these effects as increments to the baseline F-16 data set, BAR elected to add increments to the appropriate components in the model that resulted in replacement data tables. This approach maintained the same data structure in terms of the independent variables and their break points between the baseline F-16 and the VISTA configuration while significantly speeds up the process of sim-to-flight correlation. These increments are derived primarily from Wright Lab's linearized data which were obtained from Lockheed/Fort Worth as part of the VISTA simulation package. Additionally, large sideslip wind tunnel data acquired for the Peace Marble II configuration at NASA Langley's 20 ft wind tunnel were merged and utilized at upright angles of attack as illustrated in Figure 2.

The typical for all axes for the final low-speed F-16 model can be illustrated in the build-up of aerodynamic rolling moment shown below:

$$\begin{aligned}
 Cl_{\text{total}} = & Cl_{\text{basic}}(\alpha, \beta) \\
 & + DCI_{da}(\alpha, \beta * \text{SGN}(\delta A), |\delta A|) \times \text{SGN}(\delta A) \\
 & + DCI_{dr}(\alpha, \beta * \text{SGN}(\delta R), |\delta R|) \times \text{SGN}(\delta R) \\
 & + DCI_{dhh}(\alpha, \beta * \text{SGN}(\delta dh), \delta h, |\delta dh|) \times \text{SGN}(\delta dh) \\
 & + DCI_{dhr}(\alpha, (\Omega b)/(2V), \delta h_{\text{windward}}) \\
 & + CIROT(\alpha, (\Omega b)/(2V) * \text{SGN}(\beta), |\beta|) \times \text{SGN}(\beta) \\
 & + DCI_p(\alpha) \times (P_{\text{mod}} b)/(2V) \\
 & + DCI_R(\alpha) \times (R_{\text{mod}} b)/(2V)
 \end{aligned}$$

The total lateral characteristics are composed of the basic lateral stability, contributions from control surfaces, rotary (wind axis rotation), and forced oscillation (body-axis damping) terms. Known nonlinear aerodynamic characteristics and coupling effects between sideslip angle and control surface deflections from wind tunnel data were incorporated in the data tables.

Simulation / Flight Test Correlation - "Overdrive"

For the validation of the new low-speed aerodynamic model, time histories of the VISTA/MATV flight test results were obtained from Wright Lab. These flight data included test points taken from MATV flights no. 89, 94, and 100 as well as some functional check flight departures of the VISTA configuration with thrust vectoring disabled.

One of the flight test validation tools used in the simulation environment used in this analysis, "Overdrive", allows the validation of simulation aerodynamic database against flight-extracted data using the process illustrated in Figure 3.

At each time slice, extraction of aerodynamic moment coefficient from flight-recorded time history occurs as shown on the right side of Figure 3. Angular rates are numerically differentiated to obtain the angular acceleration of the vehicle. After the removal of the inertial effects and other external forces and moments such as thrust vectoring, the remainder is non-dimensionalized to calculate the aerodynamic moment coefficients during flight. The translational acceleration signals from the flight time history were also processed at each time step to extract the aerodynamic forces acting on the aircraft.

Also at each time step, flight-recorded states, such as angle of attack, angle of sideslip, control surface positions, etc., are used to exercise the

aerodynamic model in accordance with the aerodynamic model specification discussed previously. Each aerodynamic model element (*i.e.*, pitching moment due elevator, pitching moment due to flap, etc.) are stored and summed as prescribed in the aerodynamic model.

By overplotting the model predicted coefficients with the flight-extracted total coefficients, differences can be easily identified. Correlating the discrepancies with the excitation of individual elements and parameters from the flight time history helps to isolate the weaknesses in the aerodynamic model.

It should be emphasized that there is no integration during an overdrive run. The states are completely restricted to the values from the time history. The advantage of this approach is that there is no propagation of error over time. Any differences between the model-predicted and the flight-extracted values are strictly the result of local error. This "analog-matching" approach alleviates the problem associated with the propagation of error over time; any noise or drop-out of signals would not affect the analysis of the subsequent events in the time history. Additionally, flight control system is by-passed in this methodology thus avoiding any confusion between the error caused by aerodynamic modeling and the error from the flight control system model. Once the user is satisfied with aerodynamic model, the entire simulation (including aerodynamic model and flight control system modeling) can be validated by running the simulation in open-loop controlled by the flight-recorded control surface or pilot input time history.

An example of this methodology is the overplot of the sim-predicted and flight-extracted yawing moment coefficient during flight 89-02068 as shown in Figure 4. The test vehicle was stabilized at $35^\circ\alpha$ while performing a steady sideslip to $-20^\circ\beta$ as shown in the lower-left plot.

The first (upper-left) plot compares the simulation-predicted total yawing moment against the flight-extracted total yawing moment. The close correlation between the two curves validates the aerodynamic yawing moment model for the baseline VISTA configuration at these flight conditions.

Individual elements of the simulation's yawing moment can also be plotted (upper-right) to help identify the source of any mismatch between the sim-predicted and the flight-extracted aerodynamic

yawing moment coefficient. Here, the static directional stability (C_n _basic) and the incremental yawing moment due to rudder deflection (DC_n _dr) are shown.

Finally, the time history of the flight test control surfaces are shown in the 4th (lower-right) plot.

VISTA's Post-Stall Lateral Characteristics

A positive static offset was observed in the wind tunnel data and was incorporated in the initial aerodynamic model. However, the flight test data revealed a negative static rolling moment bias, thus prompting the need to mirror the nonlinear static lateral stability (C_l _basic) along with the zero sideslip offset to reflect the flight test vehicle's lateral characteristics in the 35° to $45^\circ\alpha$ range.

The flight test points in the 35 - 37.5° region indicated the VISTA configuration's ability to stabilize at large negative sideslip angles (in excess of $-15^\circ\beta$) with little roll control input while consistently demonstrated the vehicle's inability to stabilize at positive sideslip angles greater than $+5^\circ\beta$. This observation lead to the reduction of VISTA's lateral stability in the 35 - 37.5° angle of attack range to nearly neutral for negative sideslip angles as shown in Figure 5. While the original wind tunnel data exhibited some asymmetry due the sign of sideslip induced by the offset, the flight extracted asymmetry was more pronounced, albeit not unreasonably so based on other wind tunnel results of the F-16 configuration. Because of the nearly neutral lateral stability at negative sideslip, no rolling moment from the roll control surfaces (*i.e.*, flaperons, and differential tails) were required to maintain a wings-level attitude when attempting to achieve large negative sideslip excursions (Figure 6). However, the stable lateral characteristics at positive sideslip range coupled with the reduced roll authority available to the flight control system in the stall region permitted less than 5° of stabilized sideslip excursion (Figure 7).

Post-Stall Normal Force Characteristics

The correlation of normal force coefficient between the flight test data and the model-predicted values revealed significant differences in the region between 22.5 to $50^\circ\alpha$. This difference is clearly seen in Figure 8 where the comparison of sim-predicted and flight-extracted normal force coefficient are shown in the upper left plot. The individual components of the simulation normal force coefficient are plotted on the upper-right hand corner while the

horizontal stabilators and the pitch nozzle's deflection time history are shown in the lower right hand corner.

Besides the basic normal force, no other normal force components were significantly excited and virtually neutral stabilator and pitch nozzle deflections were seen during the flight. The differences can only be attributed to the basic normal force (CNf_basic) of the VISTA configuration. Based on thorough evaluation with many sets of time histories in flights 89, 94 and 100, the basic normal force coefficient is reduced in the stall/post-stall region to model the values seen in the flight test data. A comparison of the VISTA's baseline normal force coefficient between the original and the revised data set is shown in figure 9 for $0^\circ\beta$. The difference of 0.2 to 0.3 is seen throughout the stall region across a wide range of sideslip angles. It should be noted that this discrepancy between flight test and wind tunnel normal force has been observed and accounted for in other flight test evaluations (e.g. Reference 7).

Validation and Verification of Low-speed Model

Once the aerodynamic model was satisfactorily validated against the available flight test results using the overdrive methodology, simulations of the maneuvers performed during flight were conducted. Pilot input time history recorded during the flight test were used as inputs to the flight control system model (Reference 8) while exercising the new aerodynamic model. In Figure 9, the new model responses are plotted with the results of the original Wright Lab aerodynamic model simulation and compared against the recorded behavior of the flight test vehicle. Since only the aerodynamic model differed between the two sets of simulation, the close match clearly demonstrates the improved fidelity of the new aerodynamic model.

Conclusions

This paper has documented the method and data used in the development of a new low-speed aerodynamic model for the F-16/VISTA configuration. The approach taken was to use the underlying data dependencies as dictated by the wind tunnel data to build a continuous, non-linear model. The use of high angle of attack flight test data as a simulation validation and database update tool was demonstrated using an interactive method to quickly assess many flight test points. The satisfactory correlation between the flight-extracted aerodynamic coefficients and the model-predicted values clearly demonstrates that aerodynamic characteristics in the stall and post-stall region can be accurately modeled.

This was accomplished by the preservation of non-linear characteristics from the wind tunnel results in the simulation model structure. Further, the clearly defined and continuous aerodynamic model structure permitted expeditious identification of the components that caused any mismatch between the model and the flight results and allowed easy model update as dictated by flight test extraction.

References

1. Ralston, John, "F-16 NSI Inlet Configuration Study, Including Data, Analysis, Aerodynamic Math Modelling and Simulation", BAR 89-1, November 1989.
2. Ralston, John, "Analysis of High Angle of Attack Data and Simulation Results for the F-16 MCID Configuration, Including the Effects of Selected Stores", BAR 89-12, September, 1989.
3. Mason, Alvin, "F-16 Peace Marble II Rotary Balance Test Report", BAR 89-6, May, 1989.
4. Mason, Alvin, "Simulation Results for the Basic Peace Marble II and the Peace Marble II with a 300 Gallon Centerline Tank", BAR 89-10, September 1989.
5. Ralston, John, and O'Connor, Cornelius, Analysis of High Angle of Attack Data and Simulation Results for the F-16 Block 40 Configuration, Including the Effects of Selected Stores", BAR 90-10, November 1990.
6. Kalviste, Juri: Use of Rotary Balance And Forced Oscillation Test Data In A Six Degrees Of Freedom Simulation, AIAA Paper 82-1364, August 1982.
7. Sanctuary, G. E., *F-16 Flight Test Aerodynamic Coefficient Extraction Procedures and Results*, General Dynamic/Fort Worth Division, Report 16PR2405, July 15, 1982.
8. Baxter, J. S., et Al. "Flight Test & Demonstration Report for the F-16 Multi-Axis Thrust Vectoring Program." WL-TR-95-3086, January 1995.

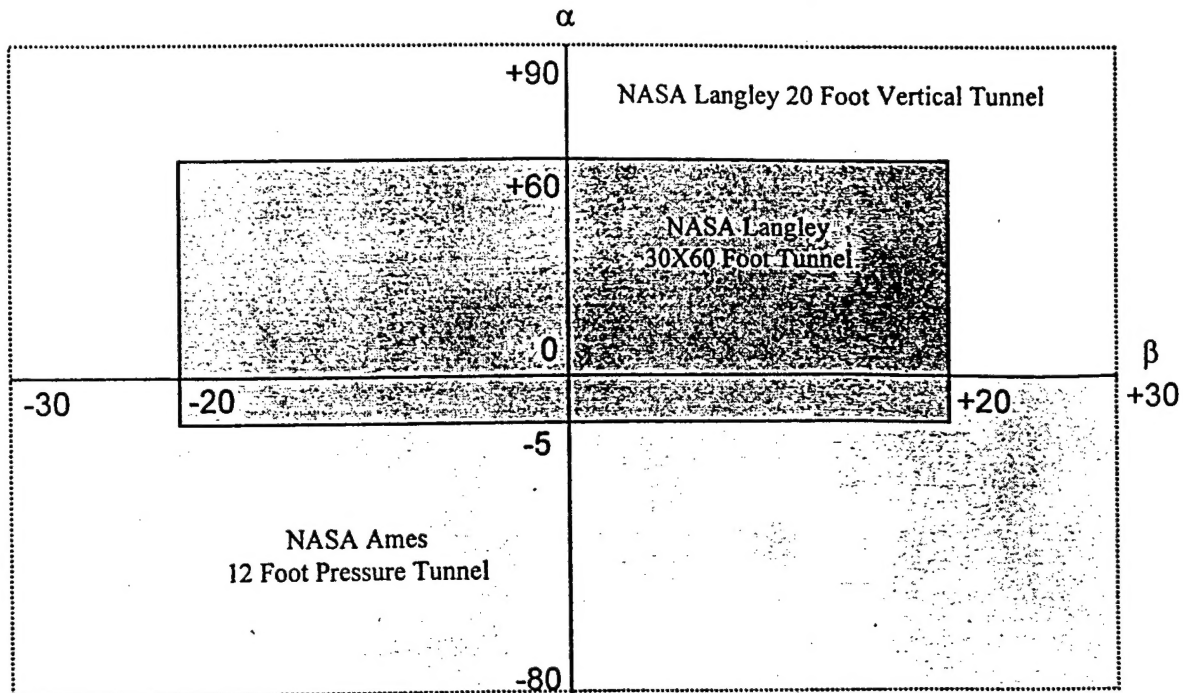


Figure 1. Database ranges for F-16's basic static aerodynamic data.

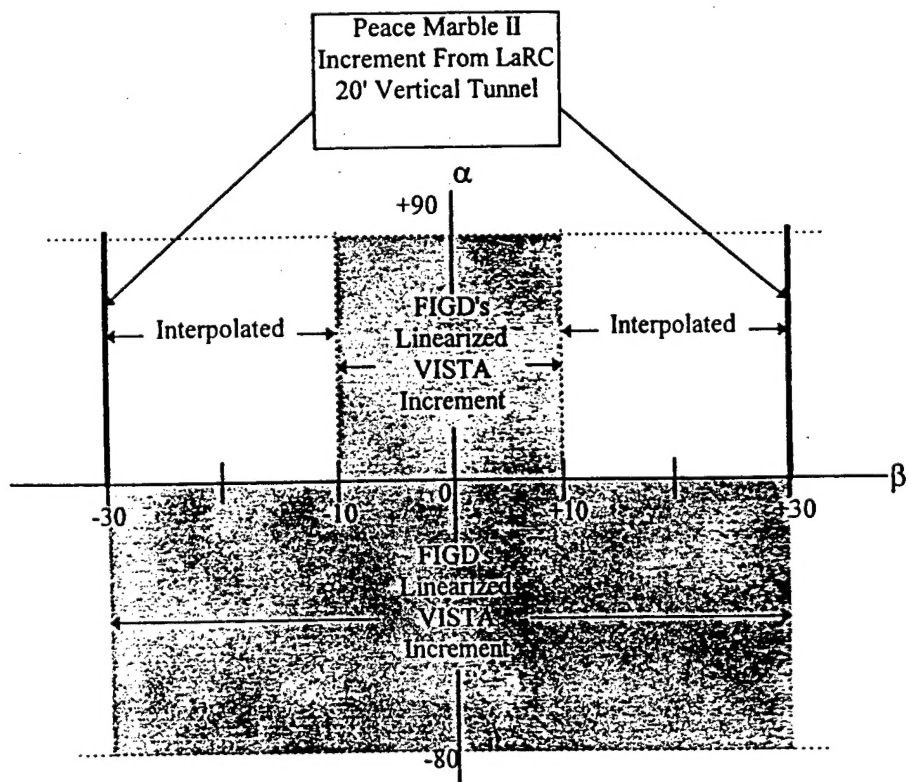


Figure 2. Data base range of the VISTA increments.

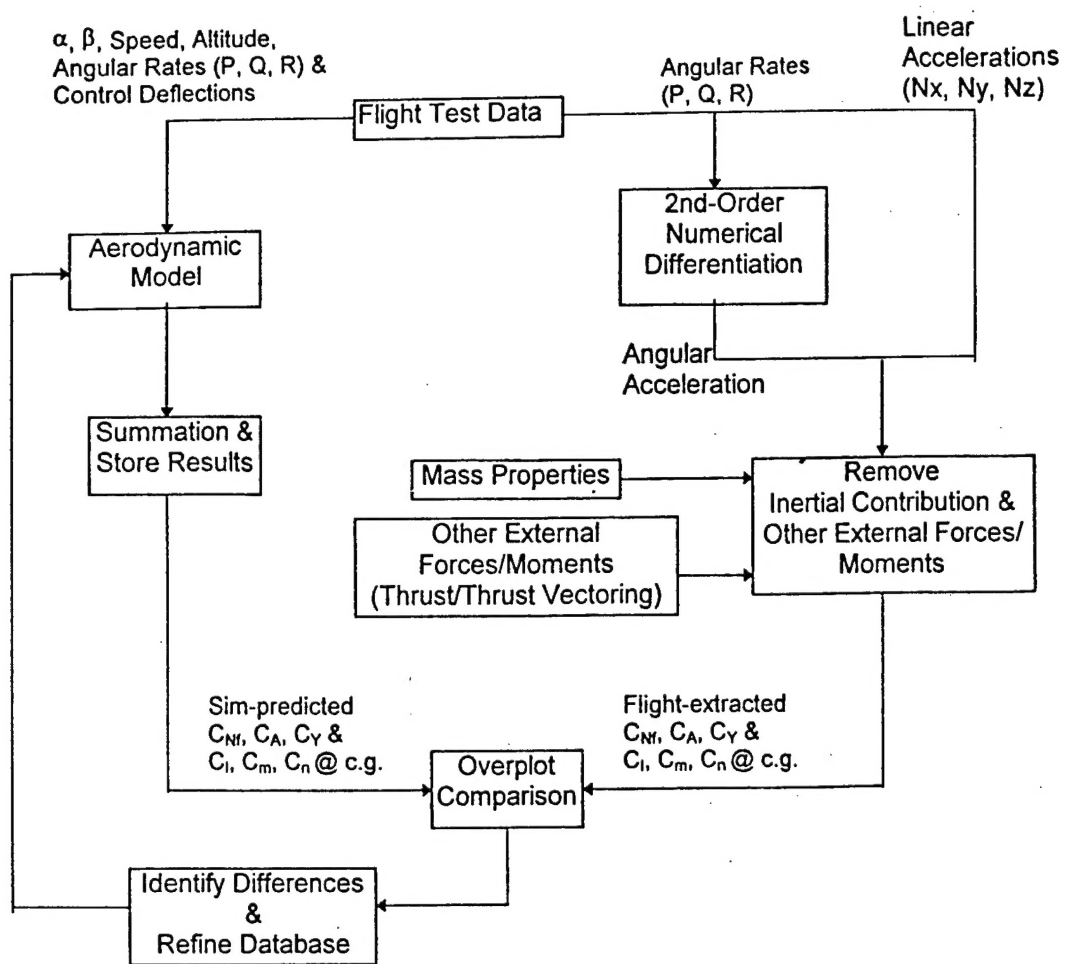


Figure 3. "Overdrive" block diagram.

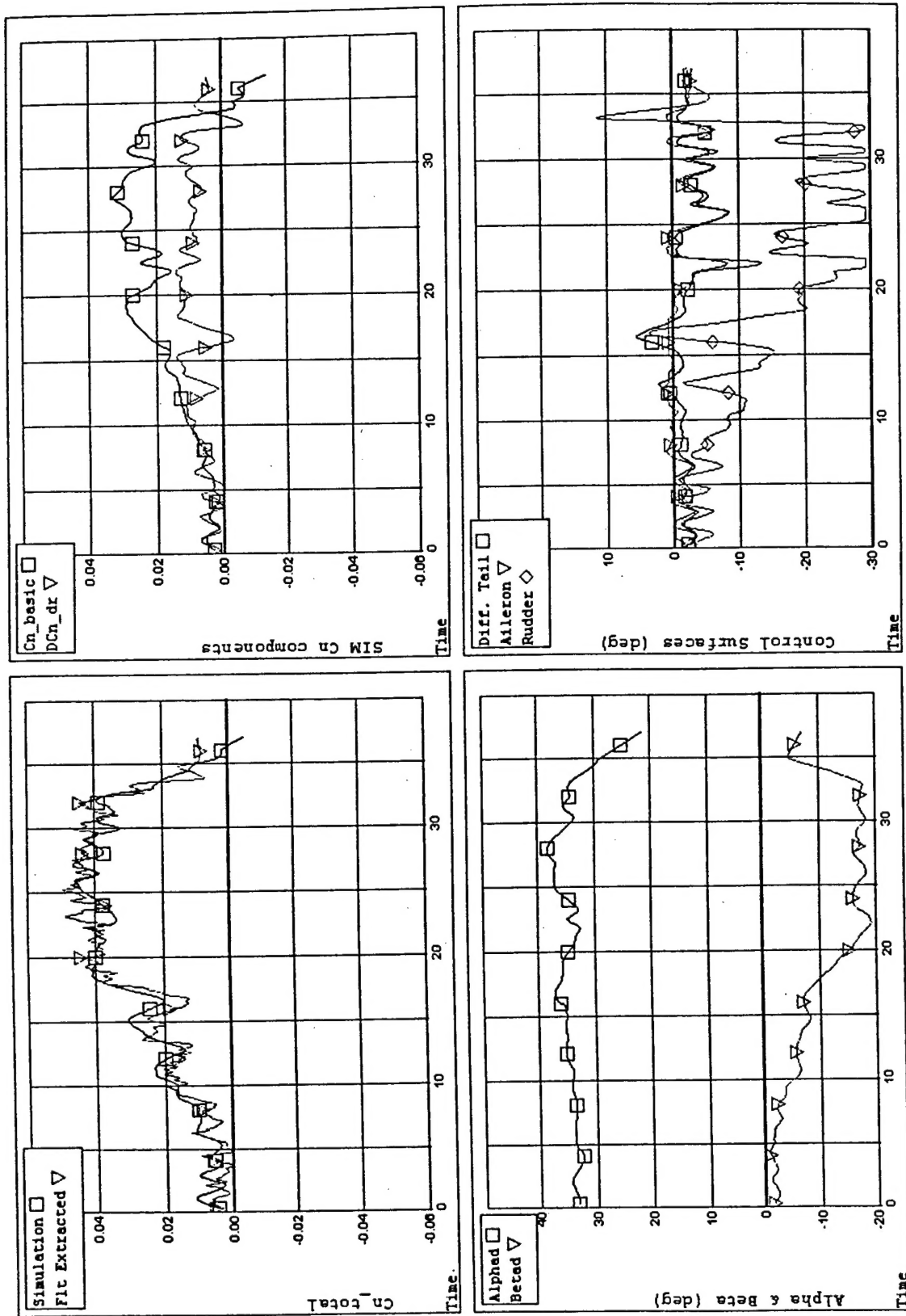


Figure 4. An example of "Overdrive" output comparing flight-extracted yawing coefficient against sim-predicted value for FLT 89-02068.

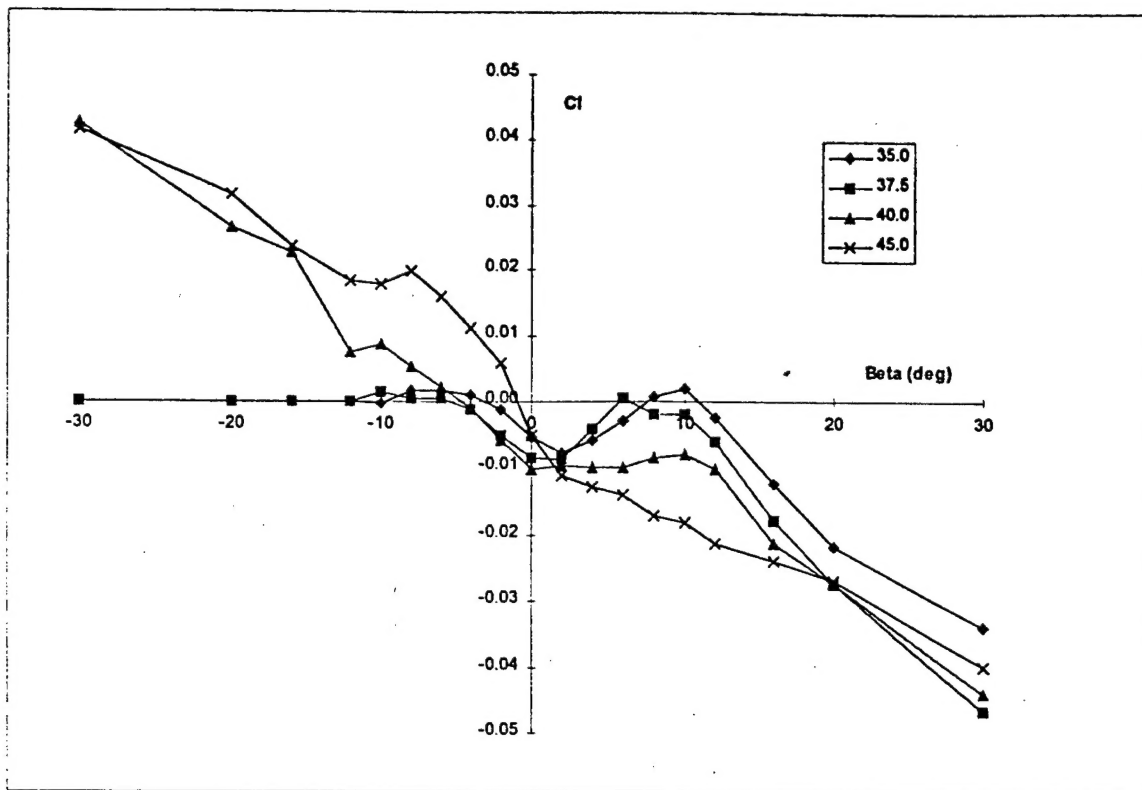


Figure 5. VISTA model's final basic static rolling moment characteristics (C_l _basic) in the stall region.

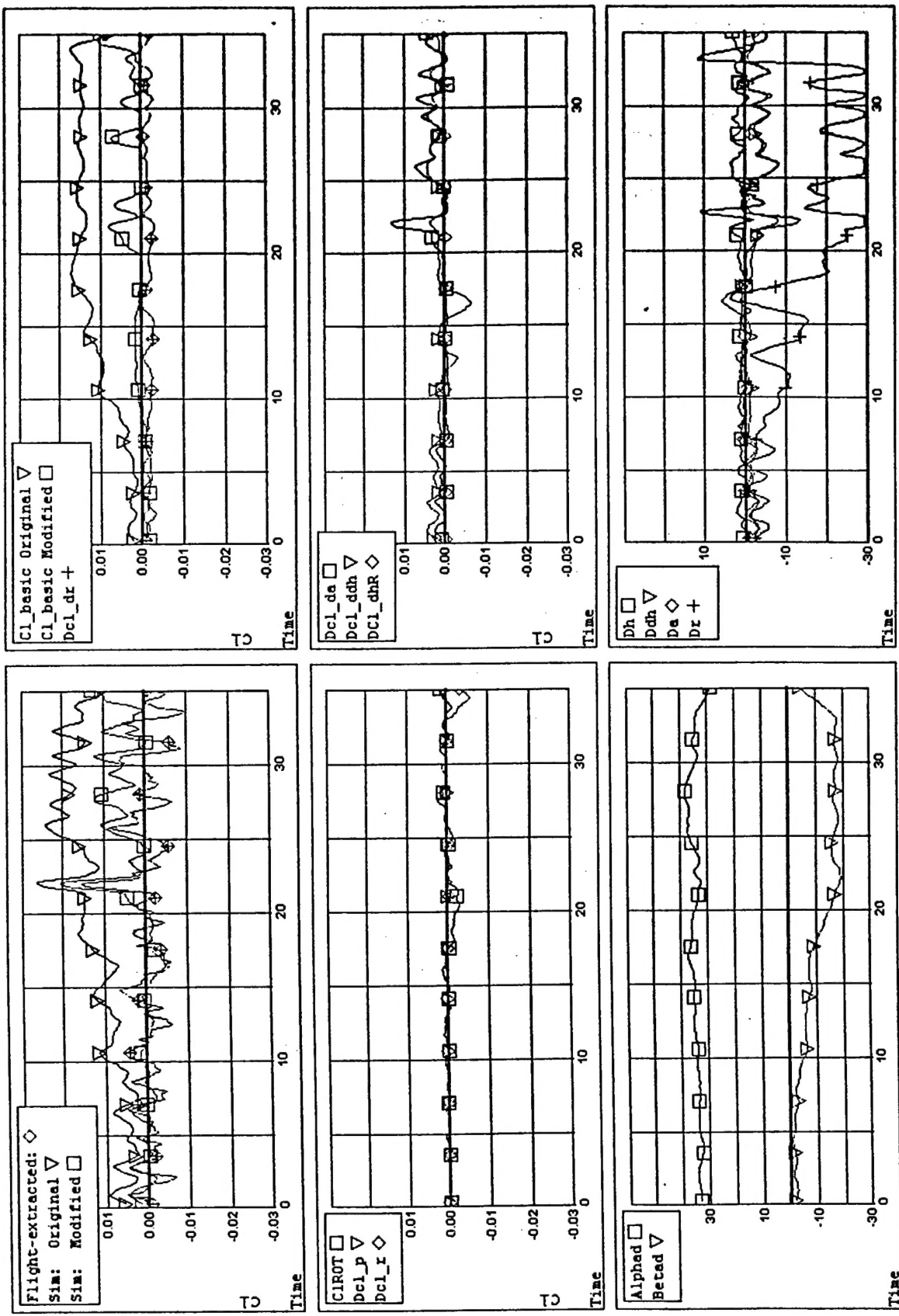


Figure 6. Comparison of sim-predicted Cl against flight-extracted values for FLT 89-02068.

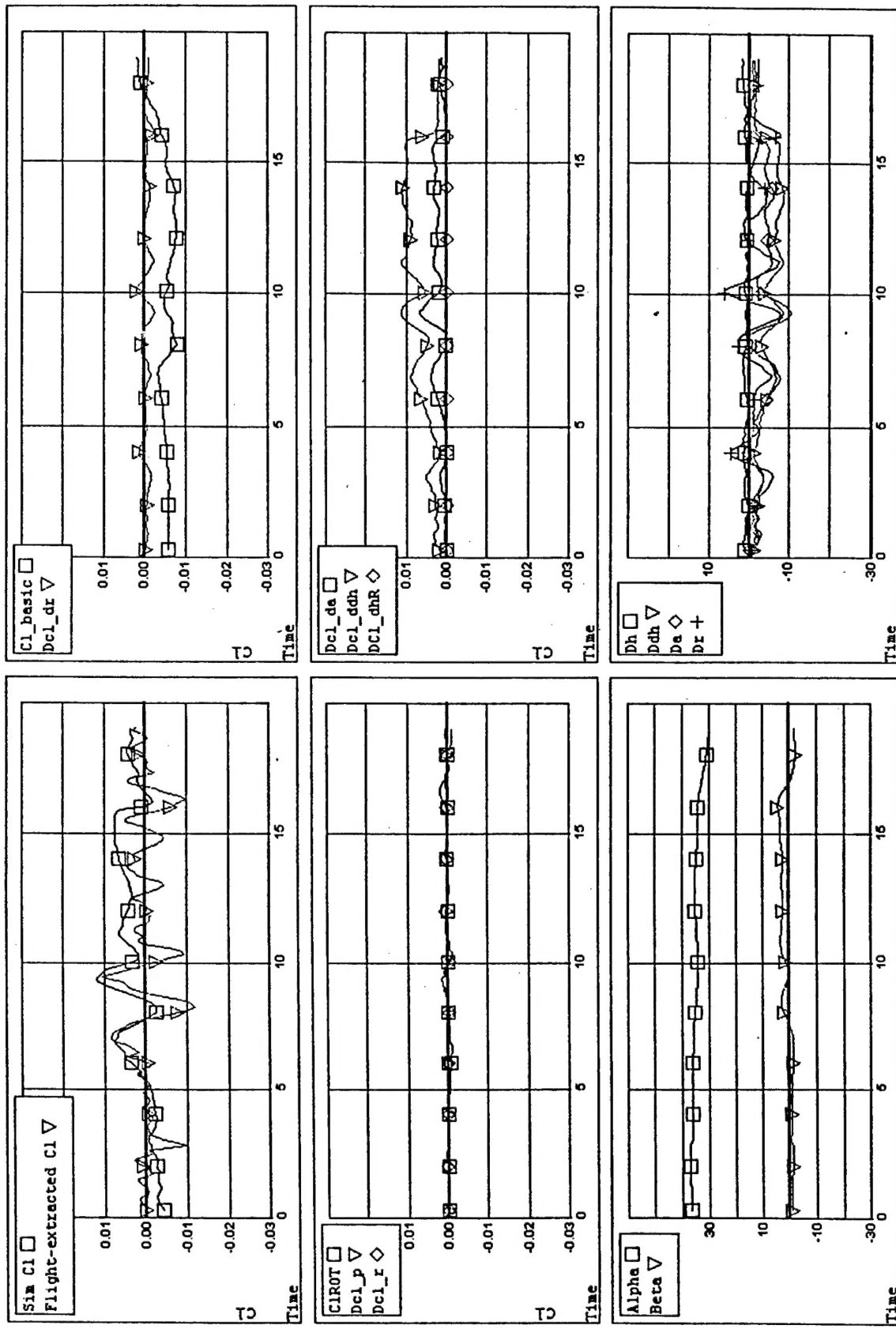


Figure 7. Comparison of sim-predicted CI against flight-extracted values for FLT 89-02040.

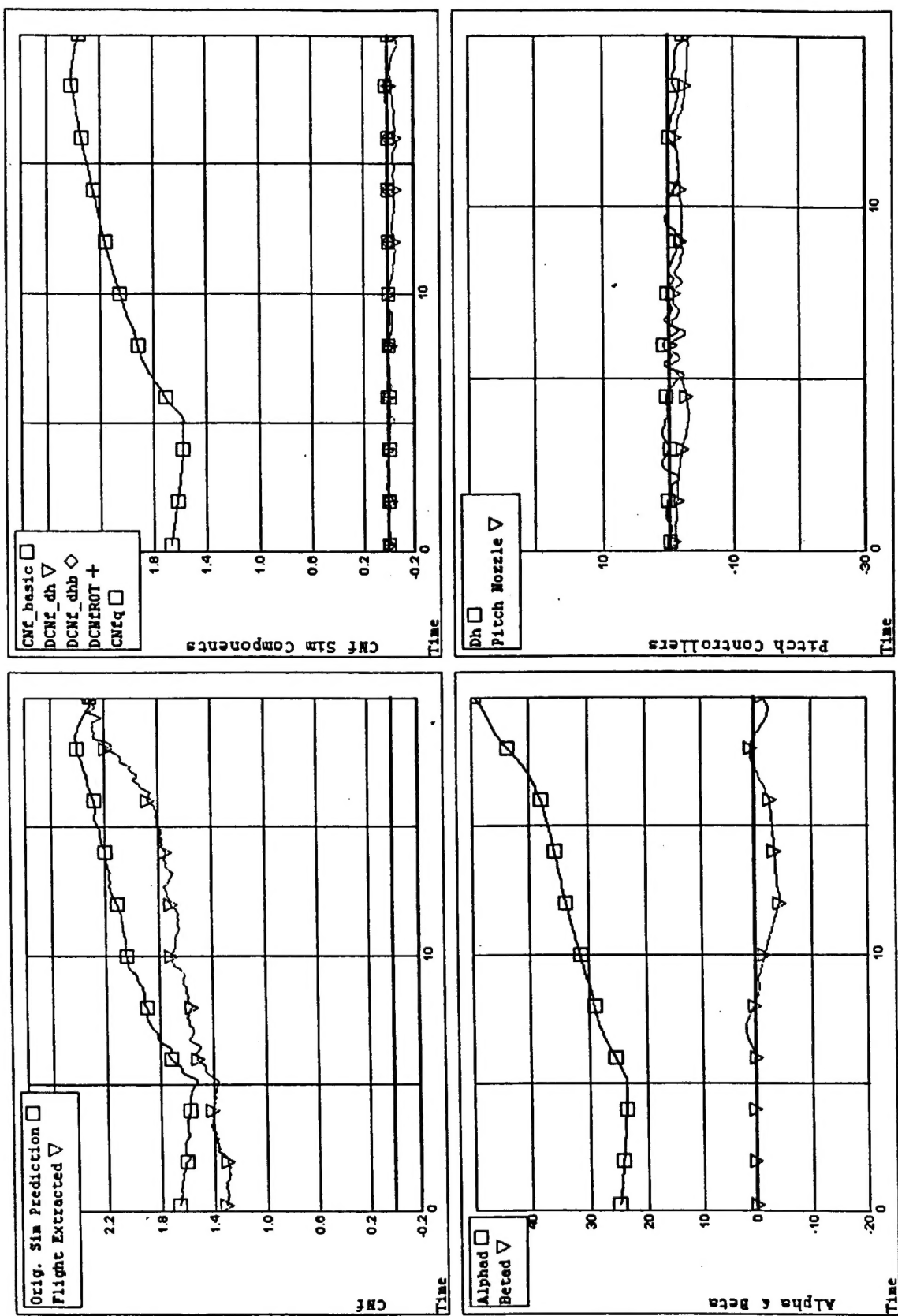


Figure 8. Comparison of sim-predicted normal force coefficient (CnF) against flight-extracted values for FLT 89-84810.

Comparison of Normal Force Coefficient

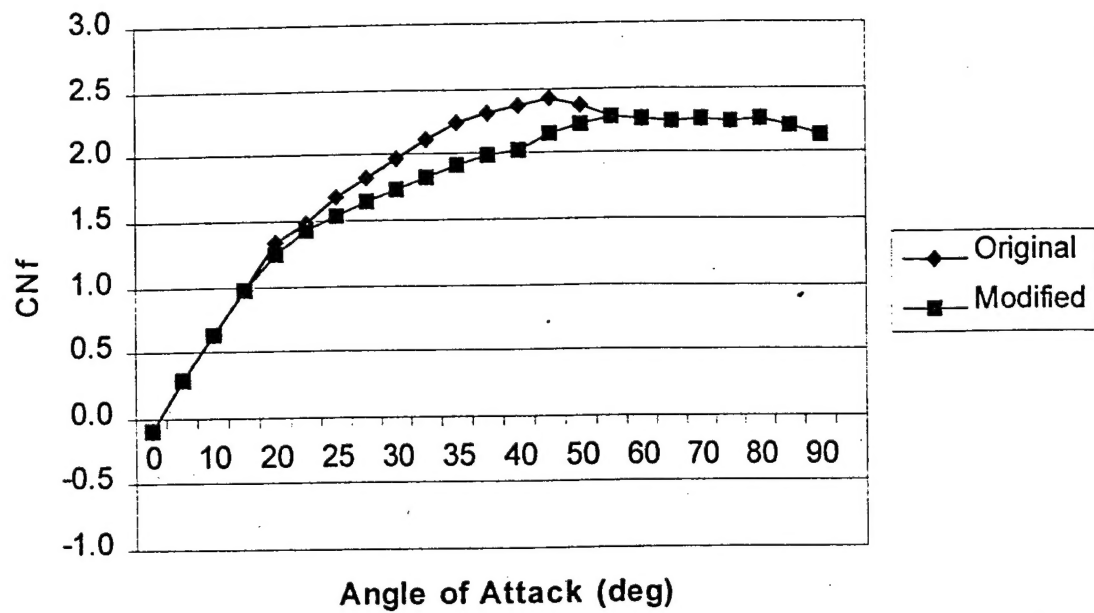


Figure 9. Comparison of the original and the modified normal force coefficient for the F-16 data base.